



# Reduced Heterochromatin Formation on the pFAR4 Miniplasmid Allows Sustained Transgene Expression in the Mouse Liver

Marie Pastor, Mickael Quiviger, Julie Pailloux, Daniel Scherman, Corinne Marie

## ► To cite this version:

Marie Pastor, Mickael Quiviger, Julie Pailloux, Daniel Scherman, Corinne Marie. Reduced Heterochromatin Formation on the pFAR4 Miniplasmid Allows Sustained Transgene Expression in the Mouse Liver. *Molecular Therapy - Nucleic Acids*, 2020, 21, pp.28-36. 10.1016/j.omtn.2020.05.014 . hal-03295373

**HAL Id: hal-03295373**

**<https://cnrs.hal.science/hal-03295373>**

Submitted on 10 Sep 2021

**HAL** is a multi-disciplinary open access archive for the deposit and dissemination of scientific research documents, whether they are published or not. The documents may come from teaching and research institutions in France or abroad, or from public or private research centers.

L'archive ouverte pluridisciplinaire **HAL**, est destinée au dépôt et à la diffusion de documents scientifiques de niveau recherche, publiés ou non, émanant des établissements d'enseignement et de recherche français ou étrangers, des laboratoires publics ou privés.

# Reduced Heterochromatin Formation on the pFAR4 Miniplasmid Allows Sustained Transgene Expression in the Mouse Liver

Marie Pastor,<sup>1</sup> Mick  l Quiviger,<sup>1</sup> Julie Pailloux,<sup>1</sup> Daniel Scherman,<sup>1</sup> and Corinne Marie<sup>1,2</sup>

<sup>1</sup>Universit   de Paris, UTCBS, CNRS, INSERM, 4, avenue de l'Observatoire, 75006 Paris, France; <sup>2</sup>Chimie ParisTech, PSL Research University, 75005 Paris, France

**Non-viral gene delivery into the liver generally mediates a transient transgene expression. A comparative analysis was performed using two gene vectors, pFAR4 and pKAR4, which differ by the absence or presence of an antibiotic resistance marker, respectively. Both plasmids carried the same eukaryotic expression cassette composed of a sulfamidase (*Sgsh*) cDNA expressed from the human alpha antitrypsin liver-specific promoter. Hydrodynamic injection of the pFAR4 construct resulted in prolonged sulfamidase secretion from the liver, whereas delivery of the pKAR4 construct led to a sharp decrease in circulating enzyme. After induction of hepatocyte division, a rapid decline of sulfamidase expression occurred, indicating that the pFAR4 derivative was mostly episomal. Quantification analyses revealed that both plasmids were present at similar copy numbers, whereas *Sgsh* transcript levels remained high only in mice infused with the pFAR4 construct. Using a chromatin immunoprecipitation assay, it was established that the 5' end of the expression cassette carried by pKAR4 exhibited a 7.9-fold higher heterochromatin-to-euchromatin ratio than the pFAR4 construct, whereas a bisulfite treatment did not highlight any obvious differences in the methylation status of the two plasmids. Thus, by preventing transgene expression silencing, the pFAR4 gene vector allows a sustained transgene product secretion from the liver.**

## INTRODUCTION

Successful gene therapies often require a long-lasting production of therapeutic proteins, enabling lifetime treatment of the patients. The outcome of the chosen approach depends upon various factors, including the therapeutic gene vector, the chosen promoter, and the targeted cell type. The liver is an important target organ for the treatment of genetic diseases and acquired disorders due to its function in synthesizing and secreting proteins that play a key role in various metabolic processes.<sup>1–3</sup> Furthermore, in contrast with other organs, the liver secretes active proteins that are properly processed and glycosylated, thus displaying all relevant posttranslational modifications for the treatment of some pathologies, such as lysosomal storage diseases or bleeding disorders. Delivery of therapeutic genes into hepatocytes can be performed by the means of either viral or non-viral vectors.<sup>1–3</sup> The most common non-viral gene vectors are plasmids that present the advantages of being easily manufactured and pro-

duced using Good Manufacturing Practices (GMP) in a cost-effective manner. In general, plasmids are composed of a eukaryotic expression cassette linked to bacterial sequences such as an origin of replication and an antibiotic resistance gene used for plasmid propagation and selection of *Escherichia coli*-containing plasmids, respectively.

Several articles reported that these prokaryotic sequences tend to promote a decrease in transgene product levels shortly after plasmid delivery to the liver, despite the fact that plasmid DNAs are still present in the transfected cells.<sup>4</sup> First, it was established that a covalent linkage between the prokaryotic DNA elements and the eukaryotic expression cassette was required to mediate transgene silencing events.<sup>5</sup> Second, a complete removal of the bacterial sequences from infused DNA sequences, using minicircles that are gene vectors composed of only a eukaryotic expression cassette, mediated a higher (until 3 log) and sustained (for at least 3 months) transgene expression, in comparison with their plasmid counterparts.<sup>6</sup> From these results, it was hypothesized that silencing events are first initiated in the bacterial plasmid backbone and subsequently spread out to the eukaryotic sequence, thus finally mediating transgene transcriptional shutdown.

Although some clues for the decline of transgene products to low or potentially basal levels were provided over the last two decades, the underlying molecular mechanisms have yet to be fully disclosed. In eukaryotes, a series of events are thought to be involved in transgene expression silencing, such as DNA methylation. This process occurs at cytosine residues that precede a guanine mainly in eukaryotic coding sequences and in promoter regions of transcriptionally inactive genes. By protruding into the DNA major groove, methyl groups act by occluding the binding of transcription factors and other proteins around the transcription initiation sequences.<sup>7</sup> In addition, proteins with a methyl CpG-binding domain (MBD), also called “readers” of methylated DNA, recruit *in situ* chromatin remodelers

Received 1 April 2020; accepted 14 May 2020;  
<https://doi.org/10.1016/j.omtn.2020.05.014>.

**Correspondence:** Corinne Marie, UTCBS, INSERM U1267, CNRS UMR8258, Facult   des Sciences Pharmaceutiques et Biologiques, 4, avenue de l'Observatoire, 75006 Paris, France.

**E-mail:** [corinne.marie@parisdescartes.fr](mailto:corinne.marie@parisdescartes.fr)

such as histone deacetylases and methylases, and finally mediate transgene expression silencing.<sup>7</sup>

In eukaryotic cells, the chromatin, the material comprising the chromosomes, can be either in an open state called the euchromatin or in a closed condensed state referred to as the heterochromatin. DNA compaction prevents the transcriptional machinery and most binding proteins from accessing DNA sequences, thus causing their transcriptional silencing. The structural units of chromatin are nucleosomes that consist of  $\approx 146/7$  bp of DNA coiled around an octameric complex composed of a pair of each of the four basic histone proteins: H2A, H2B, H3, and H4. Histone H1 is present at the surface of the nucleosome and locks the DNA wrapped around the histone core. The N-terminal ends of individual histones protrude from the globular nucleosomes and are subjected to post-translational modifications (PTMs), including lysine acetylation, arginine and lysine methylation, lysine sumoylation, or serine phosphorylation.<sup>8</sup> The acetylation and methylation of lysine residues of histones H3 and H4 probably represent the most important PTMs modulating gene expression.<sup>9,10</sup> Lysine acetylation of histones disrupts nucleosome association and favors chromatin opening up and transcriptional activation. Besides being acetylated, three methylation states of the  $\epsilon$ -amine groups of lysine residues are possible: monomethylation, dimethylation, or trimethylation. Hallmarks of heterochromatin and transgene silencing are characterized by the trimethylation of histone 3 lysine 9 (H3K9me3), histone 3 lysine 27 (H3K27me3), or histone 4 lysine 20 (H4K20me3).<sup>8,11</sup> Conversely, transcriptional activation is characterized by the H3K4me2/3 mark.<sup>8</sup> Thus, the site of methylation on histones has a major impact on the outcome of gene expression.

In order to improve transgene expression after non-viral gene delivery, we designed a small gene vector, called pFAR4, that is free of an antibiotic resistance marker. The pFAR4 miniplasmids encode a suppressor tRNA that suppresses a lethal mutation introduced into an essential gene of *E. coli*, allowing plasmid production in the absence of antibiotics.<sup>12</sup> Furthermore, the reduced size of the pFAR4 vector results in an increased transfection efficiency in all human and animal cells tested so far.<sup>12–14</sup> In the mouse liver, the hydrodynamic injection of a pFAR4 vector carrying the *N*-sulfoglucosamine sulfohydrolase (*Sgsh*) cDNA under the control of the human alpha-antitrypsin (hAAT) liver-specific promoter led to a sustained secretion of the sulfamidase protein for at least a month. In marked contrast, a fast decline occurred when the same eukaryotic expression cassette was delivered using a kanamycin-resistant plasmid (pKAR4) as a carrier.<sup>13</sup>

The objective of the present work was to extend this comparative analysis and decipher the underlying mechanisms occurring in mouse livers infused with either the pFAR4 or pKAR4 plasmid construct. Our studies include a quantification of plasmid and *Sgsh* transcript copy numbers, and an examination of heterochromatin and euchromatin marks and of the methylation status. We report that heterochromatin formation is more limited on the pFAR4 construct than on the pKAR4 plasmid, which can explain the sustained transgene expression observed with the pFAR4 vector in the liver.

## RESULTS

### Prolonged Transgene Expression after Delivery of pFAR4 Construct Does Not Result from Plasmid Integration

For this study, two plasmids containing an identical expression cassette composed of a *Sgsh* cDNA encoding the murine sulfamidase protein under the control of the hAAT liver-specific promoter were hydrodynamically injected via the tail vein of wild-type mice. The two gene vectors contain the same origin of replication and multiple cloning site (MCS) but different selection markers. The pFAR4 derivative is free of any antibiotic resistance gene, whereas the pKAR4 derivative confers resistance to kanamycin. The two plasmids, designated thereafter as pFAR4-hAAT-SGSH and pKAR4-hAAT-SGSH, have a size difference of around 1 kb, the pFAR4 vector being smaller than pKAR4 (Figure 1A).

The first comparative analysis consisted in quantifying the serum sulfamidase activity at different time points after injection of an equimolar amount (46.5 pmol) of each plasmid. Two days after plasmid injection, the serum sulfamidase activity values were with both plasmids between 16 and 20 times higher than that of wild type (Figure 1B; see also Table S1). With the pKAR4 construct, a sharp decrease in the serum enzymatic levels was observed as early as 5 days after plasmid injection, while it remained 11.3-fold higher than the wild-type value at day 145 (D145), when the mice were injected with the SGSH-encoding pFAR4 vector. Consequently, the area under the curve (AUC) determined with the antibiotic-free miniplasmid between D40 and D145 was 4.2 times higher than with the pKAR4 derivative (Figure 1C).

In an attempt to start deciphering the underlying mechanisms governing *in vivo* transgene expression, our first objective was to determine whether the beneficial effect of the pFAR4 plasmid could result from transgene integration into the genome of host cells. In order to test this hypothesis, carbon tetrachloride was intraperitoneally injected into a subgroup of mice infused with pFAR4-hAAT-SGSH at D41 after plasmid injection (Figure 2A). The chemically induced liver necrosis promoted cell division for organ regeneration and generated a sharp decrease in serum sulfamidase activity, which nearly reached basal level. Consequently, the AUC determined between D47 and D61 was significantly higher with the control mice than with the treated mice (Figure 2B). From this study, it was concluded that, upon cell division, the non-replicative pFAR4-hAAT-SGSH plasmid is not maintained in hepatocytes, suggesting that it was predominantly, if not totally, episomal (Figure 2A). Thus, in mice infused with pFAR4-hAAT-SGSH, the sustained serum sulfamidase activity does not result from plasmid integration into the mouse genome.

### pFAR4-Mediated Prolonged Serum Sulfamidase Activity Results from Higher *Sgsh* Transcript Level in the Liver

Having established that the prolonged serum sulfamidase activity mediated by the antibiotic-free plasmid did not predominantly result from transgene integration into the hepatocyte genome, our next objective was to pursue our comparative analyses between the two

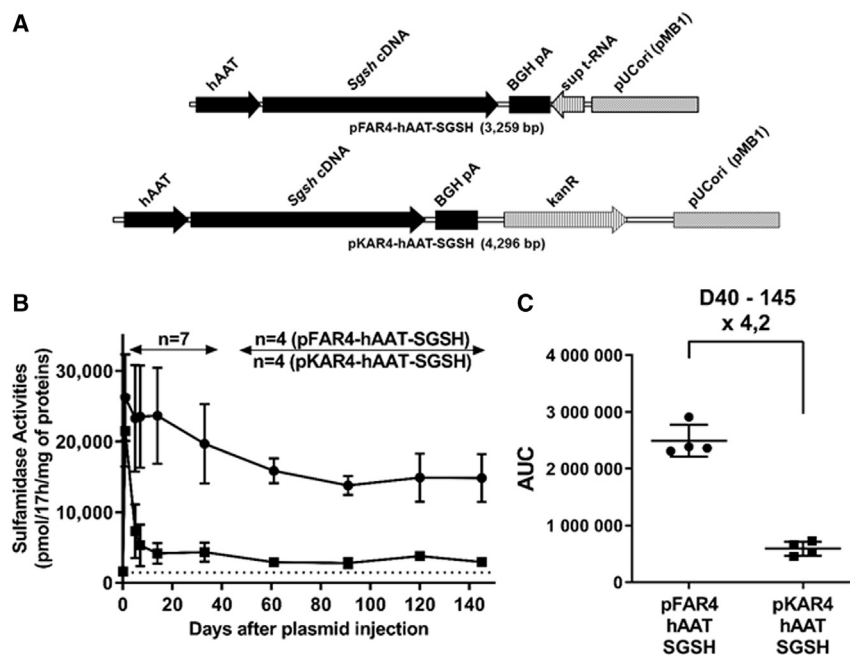


**Figure 1. pFAR4 Promotes Sustained and Elevated Serum Sulfamidase Activity**

The pFAR4 and pKAR4 derivatives contain the same eukaryotic expression cassette made of the *Sgsh* cDNA encoding the murine sulfamidase protein placed under the control of the liver-specific hAAT promoter. The plasmids contain, as a selection marker, either a kanamycin resistance gene or a suppressor (sup.) tRNA gene. The sup. tRNA is expressed from a synthetic sequence derived from the *E. coli* lipoprotein (*lpp*) promoter. This difference in the plasmid backbones reduces the size of the pFAR4 plasmid by about 1 kb (A). Hydrodynamic injection of 46.5 pmol pFAR4-hAAT-SGSH (●) into the liver of wild-type mice resulted in sustained serum sulfamidase levels, which were 11.3 times higher than wild-type values (dashed line). In marked contrast, an equimolar amount of the pKAR4 derivative (■) mediated a rapid decline of circulating sulfamidase protein (B). The Supplemental Information (Table S1) shows the results obtained at early time points after plasmid injection. The area under the curve (AUC) measured between D40 and D145 shows that the serum sulfamidase activity obtained with the pFAR4 derivative (●) was 4.2 times higher than that obtained with the pKAR4 plasmid (■) (C). Data represent mean  $\pm$  SD.

gene vectors. For each plasmid construct, mice were divided into three subgroups and were sacrificed 15, 40, and 145 days after plasmid hydrodynamic injection. We first aimed to assess whether the higher serum sulfamidase activities in mice transfected with SGSH-expressing pFAR4 could result from a superior plasmid copy number in transfected cells. Plasmid copy numbers were determined in liver extracts by quantitative polymerase chain reaction (qPCR), using a set of primers that specifically amplify a plasmid-borne region spanning the 3' end of the hAAT promoter region and the 5'-*Sgsh* cDNA sequence, and another that hybridizes with the mouse *Gapdh* (glyceraldehyde 3-phosphate dehydrogenase) sequence used for normalization (Figure 3A). The kinetic analyses revealed that plasmid copy numbers sharply decreased between D15 and D40 after plasmid injection, most probably resulting from regeneration of cells damaged by the hydrodynamic injection technique. At later time points, D40 and D145, the plasmid copy number per diploid genome tended to plateau and averaged between 4 and 9. Thus, although high sulfamidase activities were found only in sera of mice infused with pFAR4-hAAT-SGSH (Figure 1B), plasmid copy numbers in liver exhibited a similar kinetics for each gene vector (Figure 3A).

*Sgsh* transcript levels were then quantified by quantitative reverse transcription-PCR using a set of primers that hybridize on either side of the 2,589-bp first *Sgsh* intron. Results were first normalized after quantification of total cDNA amounts using primers specific to *Rpl11* encoding RNA polymerase II (RNAPII) that was identified as having the most constant expression in various tissues and being poorly affected by intra- or extra-cellular stimuli.<sup>15</sup> As early as 15 days after plasmid injection, it was already evident that transgene silencing had been initiated (Figure 3B). Indeed, the kinetic analyses

revealed that *Sgsh* transcript numbers were  $\sim$ 2,000 in pKAR4-hAAT-SGSH-transfected mice at D2 (data not shown) and reached basal levels ( $\sim$ 230) as early as D15. In marked contrast, in mice infused with the pFAR4-hAAT-SGSH construct, *Sgsh* transcript levels remained relatively constant between D40 and D145, with average values more than 14-fold higher than those measured in mice infused with pKAR4-hAAT-SGSH.

*Sgsh* transcript numbers were then normalized to plasmid copy numbers. At D15, nearly a 32-fold superior *Sgsh* transcript copy number was reached with the pFAR4-hAAT-SGSH plasmid. At D40 and D145, these values remain relatively constant and were more than 9.4-fold higher in the liver of mice infused with the pFAR4 derivative (Figure 3C). From this set of experiments, it appears that the elevated and prolonged sulfamidase activity (Figure 3D) reached with the pFAR4-hAAT-SGSH plasmid is linked to a protection from transgene expression silencing that occurs with pKAR4-hAAT-SGSH, rather than a differential loss of cells transfected with this latter plasmid.

#### Heterochromatin and Euchromatin Formation on Plasmids Hydrodynamically Injected into Mouse Livers

In order to further decipher the underlying mechanisms controlling transgene expression in the liver, we then aimed at studying the transcriptional regulatory marks present on both plasmids. In eukaryotic cells, DNA is associated with histone proteins that play an important role in the formation of either transcriptionally active euchromatin or silenced heterochromatin. One of the dynamic phenomena controlling the euchromatin/heterochromatin transition is N-terminal PTMs of the H3 proteins. Histone PTMs at specific loci can be analyzed by chromatin immunoprecipitation (ChIP) using antibodies

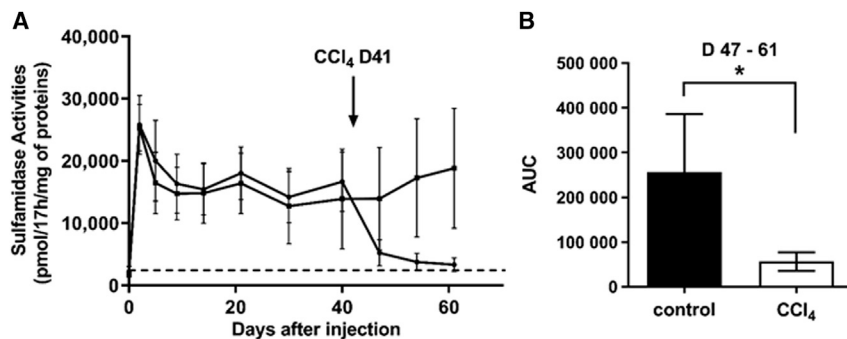


**Figure 2. Sustained Serum Sulfamidase Levels Do Not Result from Transgene Integration**

Ten wild-type mice were infused with 46.5 pmol SGSH-expressing pFAR4. Forty-one days after plasmid injection, liver cell division was induced in a subgroup of five mice by intraperitoneal injection of CCl<sub>4</sub>, whereas mice from the control group (n = 5) received only olive oil (A). The AUC was significantly different between the control and treated mice between days 47 and 61 (B). Error bars represent SD (\*p < 0.05, using the Mann-Whitney test).

that recognize specific groups present on histone proteins for a selective enrichment and coupling with qPCR for a selective amplification of targeted sequences. ChIP analyses were performed using extracts of livers from mice sacrificed 15 days after plasmid injection. The rationale for choosing this time point was dual: (1) at D15, *Sgsh* transcript levels in mice harboring the pKAR4 derivative have already reached the same minimal level as the one quantified at D40 or D145 (~200 copies per total cDNA amount); and (2) at this time point, plasmid copy number was still high, allowing the extraction of a higher chromatin amount. For the selective enrichment of chromatin fractions, three sets of antibodies were used. The first pair recognizes either heterochromatin or euchromatin marks characterized by the trimethylation of lysine 27 on histone H3 (H3K27me3) or dimethylation/trimethylation of lysine 4 on H3 (H3K4me2/3), respectively.<sup>8,11</sup> The second pair is composed of an antibody recognizing either the RNAPII protein or the phosphorylated serine 2 of the heptapeptide consensus sequence (YS<sub>2</sub>PTS<sub>5</sub>PS<sub>7</sub>) represented 52 times at the C-terminal end of RNAPII (RNAPII-Ser2P). After binding to gene promoters, RNAPII is hypo-phosphorylated. The phosphorylation of ser2 allows the formation of a stable elongation complex and represents a transcription active mark of the protein.<sup>16</sup> Third, non-immune immunoglobulin G (IgG) will be used as a negative control for the evaluation of ChIP enrichment efficiency. The mean enrichment fold for each mark was determined at two positions: (1) in the hAAT region (covering the Hepatocyte Nuclear Factor 1 $\alpha$  binding site and the transcription start site [TSS]), and (2) in the 5'-*Sgsh* cDNA end (Figure 4A).

For the H3K27me3 mark, an enrichment fold superior to 5.1 was observed when mice were infused with the pKAR4 derivative. This enrichment was observed in the hAAT promoter region (Figure 4B), as well as at the 5' SGSH end (Figure 4C). These results are in agreement with the decrease in *Sgsh* transcripts monitored in liver cells infused with pKAR4-hAAT-SGSH. Conversely, a 2.6-fold enrichment of H3K4me2/3 euchromatin mark was found to be associated with the pFAR4-hAAT-SGSH plasmid, as compared with values obtained after injection of SGSH-expressing pKAR4. Notably, a relative 3.4-fold enrichment in RNAPII-Ser2P characterizing the RNAPII elongation was also associated with the SGSH coding region carried by the pFAR4 vector. Thus, the expression cassette delivered by pFAR4 appeared to be enriched for transcription active marks, whereas the

pKAR4 vector promoted an enrichment in the H3K27me3 heterochromatin mark. This tendency was further illustrated by plotting the heterochromatin/euchromatin enrichment fold ratio, which was, with the pKAR4 construct, 7.9 times superior in the hAAT promoter region and 10.3 times higher in the 5' *Sgsh* end (Figure 4D). Thus, these results indicate that the pKAR4 vector, which contains a higher proportion of prokaryotic sequences, promotes transgene silencing via an enrichment in heterochromatin marks. In contrast, the pFAR4 vector appears to be protected from such an event.

#### Analysis of CpG Methylation

In addition to the modification of histone marks, another epigenetic mechanism involved in the silencing of eukaryotic transgene expression is DNA methylation. This process, which occurs at cytosine residues and especially in sequences rich in CpG dinucleotides clustered in promoter regions, is thought to promote heterochromatin formation. Considering that the pKAR4 construct contains a higher total number of CpG motifs (484 on both DNA strands versus 316 for the pFAR4 derivative), we compared the promoter methylation status on both plasmid constructs. The methylation status of a DNA sequence can be determined using sodium bisulfite treatment that converts unmethylated cytosine residues into uracil, while methylated cytosines are resistant to such modifications. To this end, we treated with bisulfite the same genomic DNA samples as the ones used for the evaluation of the euchromatin/heterochromatin ratio, i.e., collected 15 days after plasmid injection when transgene silencing was already evident but plasmid copy number was still high. A 438-bp fragment encompassing part of the hAAT promoter region, englobing the Hepatocyte Nuclear Factor 1 $\alpha$  and 4 binding sites, and the 5' end of the *Sgsh* cDNA sequence (Figure 5), was amplified by PCR. The sequence of individual clones was then determined and compared with that of the original plasmid. Figure 5 summarizes the results obtained following this treatment. Irrespective of the plasmid constructs, the number of sequences containing methylated cytosine residues was relatively low (mostly inferior to 10%). Although at some positions (Figure 5, b, e, j, and q) the number of methylated CpG dinucleotides seems to be higher with the pKAR4 derivative than with the pFAR4 derivative, the reverse was also observed at other positions (Figure 5, a, c, g, k, l, and o). Thus, CpG methylation could impact transgene expression in the liver, but it does not appear to be the major silencing factor at this time point.



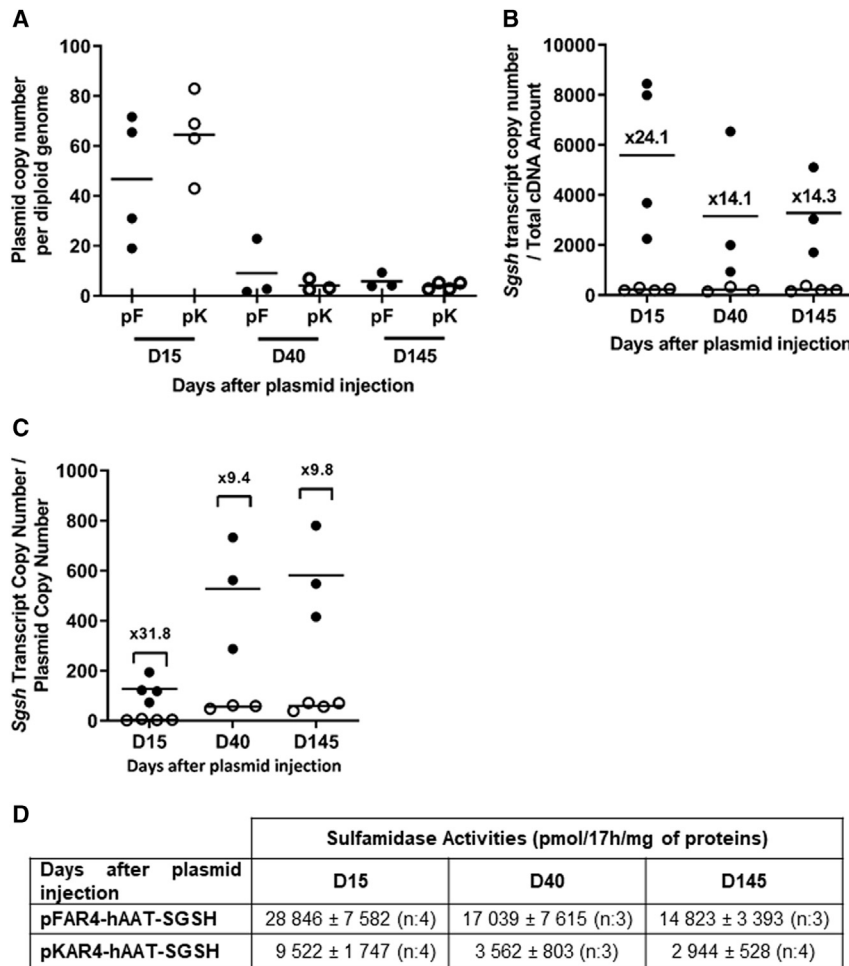


**Figure 3. High Serum Sulfamidase Activity Mediated by pFAR4-hAAT-SGSH Is Correlated to a Sustained *Sgsh* Transcript Level**

At different time points (D15, D40, and D145) after hydrodynamic injection of either pFAR4-hAAT-SGSH (●) or pKAR4-hAAT-SGSH (○), plasmid copy numbers were determined in the liver of transfected mice by using qPCR and normalized to the *Gapdh* gene (A). The *Sgsh* transcript levels quantified by qRT-PCR were either normalized to *Rpl1*, encoding RNA polymerase II (B), or to plasmid copy numbers (C). At D40 and D145, the *Sgsh* transcript level per pFAR4 plasmid copy number was more than 9.4-fold higher, as compared with the values obtained with pKAR4-hAAT-SGSH. For each time point, the serum sulfamidase activities are indicated (D), where values represent mean ± SD, and n indicates the number of mice used at each time point.

role in transgene expression silencing. By comparing the methylation status of the hAAT promoter carried by either pFAR4-hAAT-SGSH or pKAR4-hAAT-SGSH, no obvious differences were highlighted, suggesting that this event does not play a major role in transgene silencing. Still, considering the fact that the pKAR4 gene vector contains a higher number of CpG motifs than pFAR4 and the presence of a 450-bp CpG rich region identified in the 3' end of the kanamycin resistance marker, the possibility remains that these motifs interfere with gene expression via other mechanisms, such as those involving Polycomb group (PcG) proteins. PcG proteins are generally found at CpG islands or other highly

GC-enriched sequences.<sup>17</sup> Polycomb repressive complexes (PRCs), such as PRC1 and PRC2, both play a role in transgene expression silencing.<sup>18–21</sup> It is thought that PRC2 generates H3K27me3 repressive mark,<sup>22,23</sup> whereas PRC1 is important for effecting transcriptional repression by ubiquitinating H2AK119.<sup>24</sup> Notably, the insertion of GC-rich sequences originating from the *E. coli* chromosome into the genome of embryonic stem cells (ESCs) generates an enrichment in Esh2, a subunit of the PRC2 complex, and in the H3K27me3 mark.<sup>25</sup> Thus, a similar mechanism could occur on the pKAR4-hAAT-SGSH plasmid. By using a ChIP assay coupled with qPCR, a 5.1- to 6.0-fold enrichment in the H3K27me3 heterochromatin mark was highlighted, in the 5' end of the expression cassette carried by pKAR4-hAAT-SGSH. Similar results have been obtained by Gracey Maniar et al.,<sup>26</sup> who found a 5- to 15-fold H3K27me3 enrichment over the episomal plasmid as compared with a minicircle carrying the same expression cassette. Thus, after plasmid infusion, the initiation of transcription might occur from both pFAR4-hAAT-SGSH and pKAR4-hAAT-SGSH plasmids, and be at a later time point halted by negative regulation factors such as PRC2. The PRC2 proteins could bind to CpG sequences present on the pKAR4 vector, create an initial nucleation site, and subsequently methylate adjacent histone residues in

## DISCUSSION

Hydrodynamic injection of plasmids carrying the *Sgsh* cDNA expressed from the hAAT liver-specific promoter and either lacking (pFAR4-hAAT-SGSH) or containing (pKAR4-hAAT-SGSH) an antibiotic resistance marker promoted differential responses. Within a couple of weeks, the sulfamidase activity measured in the serum of mice infused with pKAR4-hAAT-SGSH declined sharply, whereas it remained high when pFAR4 was used as a gene vector. One of the goals of this study was to elucidate the underlying mechanisms. First, by inducing liver cell division, it was established that the sustained serum sulfamidase activity did not result from the integration of the eukaryotic expression cassette or of the entire injected plasmid into the hepatocyte genome. Second, the kinetic analyses also revealed that although the average amount of both plasmids was similar, transcripts from the pKAR4 construct reached basal levels as early as D15 after hydrodynamic injection, while they remained elevated with the pFAR4 derivative. These results indicated that pFAR4-hAAT-SGSH is protected from transgene expression silencing.

In mammalian genomes, several mechanisms, such as DNA methylation or heterochromatin formation, have been proposed to play a

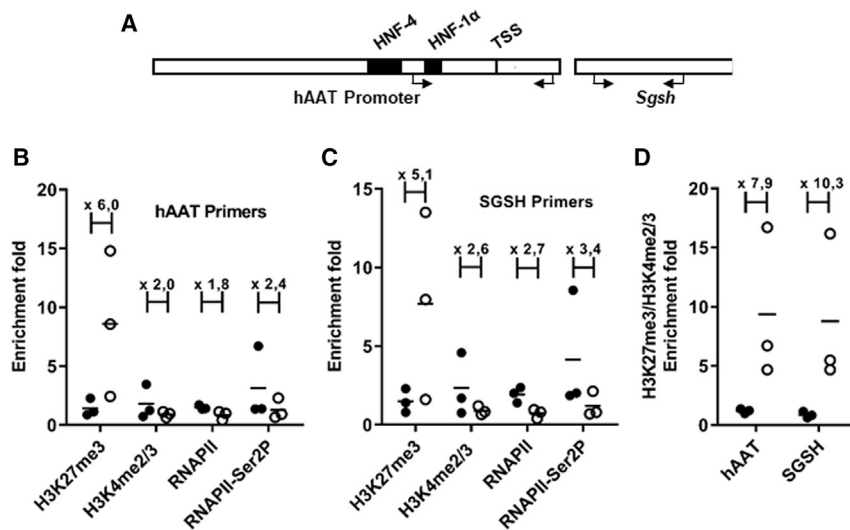


**Figure 4. Transgene Silencing Correlates with the Association of Heterochromatin Marks on the pKAR4 Plasmid**

The promoter map (A) shows transcription factor binding sites: Hepatocyte Nuclear Factor 1 $\alpha$  (HNF1 $\alpha$ ) and HNF4. The hAAT primers allow the amplification of a region covering the HNF1 $\alpha$  binding site and the transcription start site (TSS). The Sgsh primers hybridize with sequences located in the exon 1 and exon 2 regions that are separated on the chromosomal DNA sequence by a 2,189-bp intron. Antibodies recognizing either euchromatin (anti-H3K4me2/3) or heterochromatin (anti-H3K27me3) marks, the polymerase II (anti-RNAPII) or the phosphorylated serine 2 of RNAPII (anti-RNAPIISer2P), as well as non-immune IgG, were used to precipitate sonicated chromatin isolated from livers infused with either the pFAR4 (●) or the pKAR4 plasmid construct (○). Precipitated fragments were quantified by qPCR using hAAT or Sgsh-specific primers (C). The enrichment fold was calculated using the following formula:  $2^{-(C_{\text{T sample}} - C_{\text{T IgG non-immunes}})}$ , where  $C_{\text{T sample}}$  and  $C_{\text{T IgG non-immunes}}$  are the cycle thresholds ( $C_{\text{T}}$ )

obtained after immunoprecipitation using either specific antibodies or the non-immune IgG control, respectively. Both in the hAAT promoter and Sgsh regions, the heterochromatin/euchromatin ratios were with the pKAR4-hAAT-SGSH plasmid at least 7.9 times superior when compared with the pFAR4-hAAT-SGSH construct (D). For each plasmid construct, three mice were included. Each data point represents the mean of two to three independent ChIP extractions coupled with qPCR.

neighboring or more distal regions.<sup>11</sup> Indeed, by analyzing the heterochromatin/euchromatin ratio at different positions along a bacterial-viral-mammalian cell shuttle system, Suzuki et al.<sup>27</sup> found that a higher heterochromatin level was first detected in association with the bacterial sequences and subsequently spread through to the eukaryotic cassette within a few days. Thus, nucleosome spreading by information exchange could occur in a similar manner with a low turnover on the pKAR4 plasmid, whereas the pFAR4 gene vector would be protected against such an event. The two pFAR4 and pKAR4 gene vector backbones differ in several aspects: (1) pFAR4 has a smaller size (less than 1 kb) than pKAR4 (~2 kb), and (2) it contains a suppressor tRNA as a selection marker. By using a eukaryotic, non-coding DNA sequence, Lu et al.<sup>28</sup> found that the size of the DNA sequence flanking the eukaryotic expression cassette should be less than 1 kb to ascertain a sustained transgene expression. Above 1 kb, transgene expression silencing can be circumscribed by reducing the GC content of the kanamycin resistance gene from 60.6% to nearly 39% or using DNA sequences rich in AT.<sup>29</sup> The suppressor tRNA present on pFAR4-hAAT-SGSH has a GC value of 42.9%. Furthermore, it contains six AT-rich regions with a size ranging from 5 to 11 bp. Poly(dA:dT) tracts are thought to favor the exclusion of nucleosomes, thus preventing transgene expression silencing.<sup>30</sup> Thus, the pFAR4 gene vector combines the advantages of both a smaller size and a selection marker with a low GC value.

In summary, over the last two decades, considerable efforts have been made to optimize DNA non-viral gene vectors by either totally removing or reducing sequences of bacterial origin.<sup>12,31–37</sup> Undoubtedly, minicircles present the main advantage of solely being composed of a eukaryotic expression cassette. Nevertheless, their manufacturing processes remain laborious and costly because they require specific additional steps for the elimination of the prokaryotic sequences.<sup>38</sup> In contrast, pFAR4 is a user-friendly miniplasmid DNA vector into which

any fragment of interest can be introduced without any yet identified size limit. In addition, research-grade plasmid production has not faced any hurdles so far. Notably, the pFAR4 technology has been transferred successfully to a GMP facility for the production of plasmids and subsequent use in phase I/II clinical trials.<sup>39</sup> Finally, the pFAR4 efficiency has been demonstrated *in vivo* (in skin, muscle, cancer, and liver cells),<sup>12,13</sup> *in vitro* (after transfection of HeLa cells), and *ex vivo* by electroporating iris and retinal pigment epithelium<sup>14,40</sup> and CD4<sup>+</sup> and CD8<sup>+</sup> T cells,<sup>41</sup> the viability of which is negatively affected by DNA amount.<sup>42,43</sup> So far, no deleterious effect on host metabolism has been observed upon cell transfection with the pFAR4 gene vector.

Thus, the use of pFAR4 as a gene vector allows higher and sustained transgene expression levels, a reduction of required plasmid amount, and decreased production costs in comparison with other available gene vectors. The field of applications of the pFAR4 vector currently covers non-viral *in vivo* and *ex vivo* gene and cellular therapies, and could additionally be used for viral vector production.

## MATERIALS AND METHODS

### Mice

Eight-week-old female C57BL/6J mice (Janvier, Le Genest Saint Isle, France) were used for these studies that were conducted in compliance with the recommendations of the European Convention for the Protection of Vertebrates Animals used for Experimentation. Experimental protocols have been approved by the Local Ethic Committees for animal care and use.

### Plasmid Constructs and *In Vivo* Injection

The antibiotic-free pFAR4-hAAT-SGSH and kanamycin-resistant pKAR4-hAAT-SGSH plasmids contain identical eukaryotic expression cassettes composed of the murine Sgsh cDNA placed under the

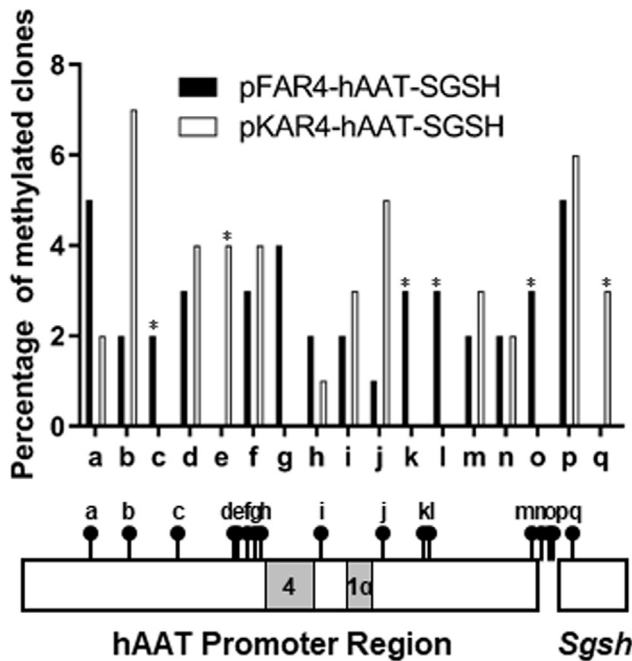


**Figure 5. Comparative Analysis of the CpG Methylation Status of the hAAT Promoter Region Carried by the pFAR4 or the pKAR4 Plasmid Constructs**

The region upstream of the *Sgsh* cDNA sequence is represented with CpG dinucleotides (●). Gray rectangles show the location of HNF1 $\alpha$  and HNF4 binding sites within the hAAT promoter region. For each plasmid construct, genomic DNA from three infused mice was treated with bisulfite. The represented DNA region was amplified by PCR. After cloning of the amplicons, 21–25 independent sequences were analyzed for each mouse. Data represent the mean of independent methylated sequences as determined by CpG retention after bisulfite treatment for each plasmid. Asterisk (\*) indicates the positions where the methylated CpG appears to be present in a plasmid sequence and absent in the other.

control of the hAAT liver-specific promoter.<sup>13</sup> Endfree plasmids were purified as described in Marie et al.<sup>12</sup> and delivered by a single hydrodynamic injection via the mouse tail vein, as described in Liu et al.<sup>44</sup> and Zhang et al.<sup>45</sup> Plasmid episomal maintenance was assessed by intraperitoneal injection of 200  $\mu$ L carbon tetrachloride 12.5% (Sigma-Aldrich) diluted in olive oil (v/v). Control mice received the same volume of vehicle (oil) intraperitoneally.

#### Quantification of Sulfamidase Enzymatic Activity

Blood samples were collected periodically by a retro-orbital technique. The sulfamidase activity was assessed using the fluorimetric substrate MU- $\alpha$ -GlcNS (4-methylumbelliferyl- $\alpha$ -D-N-sulphoglucosaminide; Carbosynth, Compton, UK), essentially as described in Karpova et al.<sup>46</sup> and Quiviger et al.<sup>13</sup>

#### Quantification of Plasmid Copy Number and *Sgsh* Transcript

Total DNA was extracted from 25 mg grounded livers harvested from mice perfused with cold phosphate buffer saline (PBS), using Phenol/CHCl<sub>3</sub>/isoamyl alcohol after an overnight cell lysis (at 56°C) in the presence of Proteinase K (0.5  $\mu$ g/ $\mu$ L) followed by an RNase A treatment (2  $\mu$ g/ $\mu$ L) at 37°C for 30 min. Plasmid DNA copy numbers

were determined by real-time PCR using an Applied Biosystems 7900HT Fast Real-Time PCR System following the recommendations provided with the Fast SYBR Green Master Mix kit (Applied Biosystems, Life Technologies, Illkirch, France). The 20- $\mu$ L reaction mixtures contained 10 ng total DNA and 500 nM each primer. The primer sequences were: pSGSH-F: 5'-AGTGAATGATCCCCCTGATCT-3' and pSGSH-R: 5'-CTCCGTCATCCGCAACTATCA-3' for plasmid quantification that was normalized with the mouse *Gapdh* sequence amplified with the following primers: gGAPDH-F3: 5'-CCTGGGATTAGGGTTGGAAAC-3' and gGAPDH-R3: 5'-GCTCAAAGGGCAAGGCTAAAG-3'. Standard amplification curves were generated using a serial dilution of plasmid templates and control mouse genomic DNA. The PCR program used was 1 min at 95°C (5 s at 95°C and 30 s at 60°C)<sub>40x</sub>, followed by a melting curve analysis of the amplified products, allowing the validation of primers specificity. The qPCRs were performed in triplicate.

Total RNAs were extracted from 10 mg grounded livers and were purified using the kit RNeasy Plus mini (QIAGEN, Courtaboeuf, France). cDNAs were synthesized at 37°C for 15 min, using 450 ng RNAs and the PrimeScript RT Master Mix kit (Takara, Ozyme, Montigny-le Bretonneux, France), in a final volume of 10  $\mu$ L. cDNA transcripts were quantified using 9 ng reverse transcribed RNA and the same conditions as those described above, using primers specific to the *Sgsh* cDNA (F: 5'-TCTGTTGGTCCTGGGACTCT-3' and R: 5'-GCGATGGCAGTGTGTGTGT-3' that hybridize on either side of the 2,589-bp intron located at 32 bp from the 5' *Sgsh* cDNA end) and to rPII (F: 5'-TAAGCCCAGTGACCTTCATC-3' and R: 5'-ATGCCCCATCATGGACATTT-3'). *RpII* encodes the RNAPII polypeptide A (Polr2a); it is used as a reference gene for this transcription analysis as displaying the most constant expression in different tissues.<sup>15</sup> Negative controls included samples treated in the absence of reverse transcriptase or using genomic DNA isolated from non-transfected mice.

#### Analysis of the Chromatin Marks Present on Plasmids Hydrodynamically Injected into the Mouse Liver

Chromatin marks on plasmids injected into mouse livers were analyzed by ChIP assays using the “High Sensitivity ChIP kit” (ab185913; Abcam, Paris, France). The chromatin was extracted from two times 10 mg grounded liver per sample. In brief, DNA and proteins were first cross-linked at room temperature for 8 min with a constant agitation, using formaldehyde (1% in PBS supplemented with protease inhibitors). The reaction was quenched by incubating the samples at room temperature for 5 min in the presence of glycine (0.125M). After three washes with PBS supplemented with protease inhibitors, samples were suspended in the lysis buffer provided with the kit. After grinding with a Potter, lysates were filtrated through a cell strainer (40  $\mu$ m; Falcon, Dutscher, Brumath, France). The chromatin pelleted by centrifugation was suspended using the provided ChIP buffer and sonicated at 4°C using a Diagenode Bioruptor Standard sonicator (UCD-200) and three rounds of five sonication cycles (30 s ON ; 30 s OFF) and the “High” Intensity setup. The sonication efficiency was validated by loading the DNA onto a 1.5%



agarose gel, after its release from proteins using the Abcam “DNA release buffer” supplemented with Proteinase K (0.4 µg/µL), a phenol/chloroform extraction, and ethanol precipitation in the presence of sodium acetate (0.3M, pH 5.2) and glycogen (50 ng/µL).

Prior to the quantification of DNA fragments linked to specific protein marks, a selective enrichment of chromatin fractions was performed by immunoprecipitation. To this end, the following antibodies (0.8 µg) were added to wells coated with the chimeric A/G protein: (1) anti-H3K27me3 (Ab6002; Abcam) and anti-H3K4me2/3 (Ab6000; Abcam) that are specific to heterochromatin and euchromatin marks, respectively; and (2) anti-RNAPolII S2-P (Ab5095; Abcam) that recognizes the phosphorylated serine found in the amino acid 2 position of the PolII C-terminal domain repeat YS<sub>2</sub>PTSPS and the anti-RNAPII (Ab185913; Abcam). As a negative control and to assess the background level, non-immune IgG antibodies (Ab185913; Abcam) were also included. After an incubation of 90 min, the wells were washed with the provided ChIP buffer. Eight micrograms of sonicated chromatin was then added to each well and incubated for 3 h at room temperature. After four washes with the “ChIP washing buffer” provided in the kit, DNAs were released from cross-linked proteins, using the “ChIP DNA release buffer” supplemented with RNase (0.25 µg/µL) and Proteinase K (0.5 µg/µL). After purification using the provided F-spin columns, DNAs were quantified by real-time PCR using primers hybridizing with either the hAAT promoter (F: 5'-ACTGGGGTGACCTTGGTTAAT-3' and R: 5'-ATCAGGGGGATCATTCACTGT-3') or the *Sgsh* cDNA sequence (F: 5'-GCCTGCTGCACAATTCTGTT-3' and R: 5'-CTCTCAAAGCCTCCGTCATC-3'), at a concentration of 0.2 and 0.5 µM, respectively. The enrichment fold was calculated using the following formula:  $2^{-(C_T^{IP} - C_T^{IgG \text{ non-immunes}})}$ , where  $C_T^{IP}$  and  $C_T^{IgG}$  are the cycle threshold values obtained after qPCRs of DNA fragments precipitated in the presence of specific antibodies or non-immune IgG, respectively.

### Analysis of CpG Methylation Status

Fifteen days after plasmid delivery, genomic DNA was extracted from the mouse liver, and 1.5 µg was treated with bisulfite using the EpiTect Bisulfite kit (QIAGEN, Courtaboeuf, France). PCR fragments (438 bp) covering the hAAT promoter and the 5'-SGSH cDNA region were then amplified using the following primers: hAAT-CpG-F2: 5'-GAGTA GAGGGTTAGTTAAGTGGTATTTTATAGAGA-3' and SGSH-CpG-R3: 5'-ATCCCAAAACCAACAAATTATACAACAAACCA A-3' and the Epimark Hot Start polymerase (New England Biolabs, Evry, France). After cloning of the amplicons, individual clones were independently sequenced. The efficiency of the bisulfite treatment ranged from 81% to 100%, as determined with the count of modified cytosine residues. For an accurate determination of the CpG methylation pattern, the clones for which the cytosine bisulfite conversion did not occur efficiently were discarded from the analysis.

### Statistical Analysis

Data were analyzed using GraphPad Prism 5 software. The significance of differences between groups was determined based on exact

two-tailed p values obtained with the nonparametric Mann-Whitney test. A p value <0.05 was considered statistically significant.

### SUPPLEMENTAL INFORMATION

Supplemental Information can be found online at <https://doi.org/10.1016/j.omtn.2020.05.014>.

### AUTHOR CONTRIBUTIONS

Investigation, Methodology, Validation, Writing – Original Draft: M.P.; Investigation, M.Q. and J.P.; Funding Acquisition, Writing – Review & Editing, D.S.; Conceptualization, Methodology, Validation, Resources, Writing – Original Draft, Writing – Review & Editing, Supervision, Funding Acquisition, C.M.

### CONFLICTS OF INTEREST

The authors declare no competing interests.

### ACKNOWLEDGMENTS

The performed work has been supported through an E-RARE ERANET grant, TRANSPOMART-E-Rare-2 JTC 2011.

### REFERENCES

- Zabaleta, N., Hommel, M., Salas, D., and Gonzalez-Aseguinolaza, G. (2019). Genetic-Based Approaches to Inherited Metabolic Liver Diseases. *Hum. Gene Ther.* 30, 1190–1203.
- McKay, T.R., Rahim, A.A., Buckley, S.M.K., Ward, N.J., Chan, J.K.Y., Howe, S.J., and Waddington, S.N. (2011). Perinatal gene transfer to the liver. *Curr. Pharm. Des.* 17, 2528–2541.
- Aravalli, R.N., Belcher, J.D., and Steer, C.J. (2015). Liver-targeted gene therapy: Approaches and challenges. *Liver Transpl.* 21, 718–737.
- Chen, Z.-Y., Yant, S.R., He, C.-Y., Meuse, L., Shen, S., and Kay, M.A. (2001). Linear DNAs concatamerize in vivo and result in sustained transgene expression in mouse liver. *Mol. Ther.* 3, 403–410.
- Chen, Z.Y., He, C.-Y., Meuse, L., and Kay, M.A. (2004). Silencing of episomal transgene expression by plasmid bacterial DNA elements in vivo. *Gene Ther.* 11, 856–864.
- Chen, Z.-Y., He, C.-Y., Ehrhardt, A., and Kay, M.A. (2003). Minicircle DNA vectors devoid of bacterial DNA result in persistent and high-level transgene expression in vivo. *Mol. Ther.* 8, 495–500.
- Du, Q., Luu, P.-L., Stirzaker, C., and Clark, S.J. (2015). Methyl-CpG-binding domain proteins: readers of the epigenome. *Epigenomics* 7, 1051–1073.
- Latham, J.A., and Dent, S.Y.R. (2007). Cross-regulation of histone modifications. *Nat. Struct. Mol. Biol.* 14, 1017–1024.
- Jenuwein, T., and Allis, C.D. (2001). Translating the histone code. *Science* 293, 1074–1080.
- Grewal, S.I.S., and Moazed, D. (2003). Heterochromatin and epigenetic control of gene expression. *Science* 301, 798–802.
- Erdel, F. (2017). How Communication Between Nucleosomes Enables Spreading and Epigenetic Memory of Histone Modifications. *BioEssays* 39, 1700053.
- Marie, C., Vandermeulen, G., Quiviger, M., Richard, M., Pr  at, V., and Scherman, D. (2010). pFARs, plasmids free of antibiotic resistance markers, display high-level transgene expression in muscle, skin and tumour cells. *J. Gene Med.* 12, 323–332.
- Quiviger, M., Arfi, A., Mansard, D., Delacotte, L., Pastor, M., Scherman, D., and Marie, C. (2014). High and prolonged sulfamidase secretion by the liver of MPS-IIIa mice following hydrodynamic tail vein delivery of antibiotic-free pFAR4 plasmid vector. *Gene Ther.* 21, 1001–1007.
- Thumann, G., Harmening, N., Prat-Souteyrand, C., Marie, C., Pastor, M., Sebe, A., Miskey, C., Hurst, L.D., Diarra, S., Kropp, M., et al. (2017). Engineering of PEDF-

- Expressing Primary Pigment Epithelial Cells by the SB Transposon System Delivered by pFAR4 Plasmids. *Mol. Ther. Nucleic Acids* 6, 302–314.
15. Radonić, A., Thulke, S., Mackay, I.M., Landt, O., Siegert, W., and Nitsche, A. (2004). Guideline to reference gene selection for quantitative real-time PCR. *Biochem. Biophys. Res. Commun.* 313, 856–862.
  16. Eick, D., and Geyer, M. (2013). The RNA polymerase II carboxy-terminal domain (CTD) code. *Chem. Rev.* 113, 8456–8490.
  17. Ku, M., Koche, R.P., Rheinbay, E., Mendenhall, E.M., Endoh, M., Mikkelsen, T.S., Presser, A., Nusbaum, C., Xie, X., Chi, A.S., et al. (2008). Genomewide analysis of PRC1 and PRC2 occupancy identifies two classes of bivalent domains. *PLoS Genet.* 4, e1000242.
  18. Laugesen, A., Højfeldt, J.W., and Helin, K. (2019). Molecular Mechanisms Directing PRC2 Recruitment and H3K27 Methylation. *Mol. Cell* 74, 8–18.
  19. Simon, J.A., and Kingston, R.E. (2009). Mechanisms of polycomb gene silencing: knowns and unknowns. *Nat. Rev. Mol. Cell Biol.* 10, 697–708.
  20. Golbabapour, S., Majid, N.A., Hassandarvish, P., Hajrezaie, M., Abdulla, M.A., and Hadi, A.H.A. (2013). Gene silencing and Polycomb group proteins: an overview of their structure, mechanisms and phylogenetics. *OMICS* 17, 283–296.
  21. van Kruijsbergen, I., Hontelez, S., and Veenstra, G.J.C. (2015). Recruiting polycomb to chromatin. *Int. J. Biochem. Cell Biol.* 67, 177–187.
  22. Cao, R., and Zhang, Y. (2004). SUZ12 is required for both the histone methyltransferase activity and the silencing function of the EED-EZH2 complex. *Mol. Cell* 15, 57–67.
  23. Pasini, D., Bracken, A.P., Jensen, M.R., Lazzerini Denchi, E., and Helin, K. (2004). Suz12 is essential for mouse development and for EZH2 histone methyltransferase activity. *EMBO J.* 23, 4061–4071.
  24. Wang, H., Wang, L., Erdjument-Bromage, H., Vidal, M., Tempst, P., Jones, R.S., and Zhang, Y. (2004). Role of histone H2A ubiquitination in Polycomb silencing. *Nature* 431, 873–878.
  25. Mendenhall, E.M., Koche, R.P., Truong, T., Zhou, V.W., Issac, B., Chi, A.S., Ku, M., and Bernstein, B.E. (2010). GC-rich sequence elements recruit PRC2 in mammalian ES cells. *PLoS Genet.* 6, e1001244.
  26. Gracey Maniar, L.E., Maniar, J.M., Chen, Z.Y., Lu, J., Fire, A.Z., and Kay, M.A. (2013). Minicircle DNA vectors achieve sustained expression reflected by active chromatin and transcriptional level. *Mol. Ther.* 21, 131–138.
  27. Suzuki, M., Kasai, K., and Saeki, Y. (2006). Plasmid DNA sequences present in conventional herpes simplex virus amplicon vectors cause rapid transgene silencing by forming inactive chromatin. *J. Virol.* 80, 3293–3300.
  28. Lu, J., Zhang, F., Xu, S., Fire, A.Z., and Kay, M.A. (2012). The extragenic spacer length between the 5' and 3' ends of the transgene expression cassette affects transgene silencing from plasmid-based vectors. *Mol. Ther.* 20, 2111–2119.
  29. Lu, J., Zhang, F., Fire, A.Z., and Kay, M.A. (2017). Sequence-Modified Antibiotic Resistance Genes Provide Sustained Plasmid-Mediated Transgene Expression in Mammals. *Mol. Ther.* 25, 1187–1198.
  30. Segal, E., and Widom, J. (2009). Poly(dA:dT) tracts: major determinants of nucleosome organization. *Curr. Opin. Struct. Biol.* 19, 65–71.
  31. Cranenburgh, R.M., Hanak, J.A.J., Williams, S.G., and Sherratt, D.J. (2001). *Escherichia coli* strains that allow antibiotic-free plasmid selection and maintenance by repressor titration. *Nucleic Acids Res.* 29, E26.
  32. Cranenburgh, R.M., Lewis, K.S., and Hanak, J.A.J. (2004). Effect of plasmid copy number and lac operator sequence on antibiotic-free plasmid selection by operator-repressor titration in *Escherichia coli*. *J. Mol. Microbiol. Biotechnol.* 7, 197–203.
  33. Soubrier, F., Cameron, B., Manse, B., Somarriba, S., Dubertret, C., Jaslin, G., Jung, G., Caer, C.L., Dang, D., Mouvault, J.M., et al. (1999). pCOR: a new design of plasmid vectors for nonviral gene therapy. *Gene Ther.* 6, 1482–1488.
  34. Soubrier, F., Laborde, B., and Cameron, B. (2005). Improvement of pCOR plasmid copy number for pharmaceutical applications. *Appl. Microbiol. Biotechnol.* 66, 683–688.
  35. Pfaffenzeller, I., Mairhofer, J., Striedner, G., Bayer, K., and Grabherr, R. (2006). Using ColE1-derived RNA I for suppression of a bacterially encoded gene: implication for a novel plasmid addition system. *Biotechnol. J.* 1, 675–681.
  36. Mairhofer, J., Cserjan-Puschmann, M., Striedner, G., Nöbauer, K., Razzazi-Fazeli, E., and Grabherr, R. (2010). Marker-free plasmids for gene therapeutic applications—lack of antibiotic resistance gene substantially improves the manufacturing process. *J. Biotechnol.* 146, 130–137.
  37. Luke, J., Carnes, A.E., Hodgson, C.P., and Williams, J.A. (2009). Improved antibiotic-free DNA vaccine vectors utilizing a novel RNA based plasmid selection system. *Vaccine* 27, 6454–6459.
  38. Chen, Z.-Y., He, C.-Y., and Kay, M.A. (2005). Improved production and purification of minicircle DNA vector free of plasmid bacterial sequences and capable of persistent transgene expression in vivo. *Hum. Gene Ther.* 16, 126–131.
  39. Bakker, N.A.M., de Boer, R., Marie, C., Scherman, D., Haanen, J.B.A.G., Beijnen, J.H., Nuijen, B., and van den Berg, J.H. (2019). Small-scale GMP production of plasmid DNA using a simplified and fully disposable production method. *J. Biotechnol.* 2, 100007.
  40. Pastor, M., Johnen, S., Harmening, N., Quiviger, M., Pailloux, J., Kropp, M., Walter, P., Ivics, Z., Izsvák, Z., Thumann, G., et al. (2018). The Antibiotic-free pFAR4 Vector Paired with the Sleeping Beauty Transposon System Mediates Efficient Transgene Delivery in Human Cells. *Mol. Ther. Nucleic Acids* 11, 57–67.
  41. Gogishvili, T., Monjezi, R., Marie, C., Machwirth, M., Einsele, H., Zoltan, I., Scherman, D., and Hudecek, M. (2017). Enhanced engineering of chimeric antigen receptor (CAR)-modified T Cells using non-viral Sleeping Beauty transposition from pFAR vectors. *Hum. Gene Ther.* 28, A32.
  42. Clauss, J., Obenaus, M., Miskey, C., Ivics, Z., Izsvák, Z., Uckert, W., and Bunse, M. (2018). Efficient Non-Viral T-Cell Engineering by Sleeping Beauty Minicircles Diminishing DNA Toxicity and miRNAs Silencing the Endogenous T-Cell Receptors. *Hum. Gene Ther.* 29, 569–584.
  43. Monjezi, R., Miskey, C., Gogishvili, T., Schleef, M., Schmeer, M., Einsele, H., Ivics, Z., and Hudecek, M. (2017). Enhanced CAR T-cell engineering using non-viral Sleeping Beauty transposition from minicircle vectors. *Leukemia* 31, 186–194.
  44. Liu, F., Song, Y., and Liu, D. (1999). Hydrodynamics-based transfection in animals by systemic administration of plasmid DNA. *Gene Ther.* 6, 1258–1266.
  45. Zhang, G., Budker, V., and Wolff, J.A. (1999). High levels of foreign gene expression in hepatocytes after tail vein injections of naked plasmid DNA. *Hum. Gene Ther.* 10, 1735–1737.
  46. Karpova, E.A., Voznyi YaV, Keulemans, J.L.M., Hoogeveen, A.T., Winchester, B., Tsvetkova, I.V., and van Diggelen, O.P. (1996). A fluorimetric enzyme assay for the diagnosis of Sanfilippo disease type A (MPS IIIA). *J. Inher. Metab. Dis.* 19, 278–285.